Granular Matter (2021) 23:57
https://doi.org/10.1007/s10035-021-01125-2

ORIGINAL PAPER

Influence of bottom roughness and ambient pressure conditions on the emplacement of experimental dam-break granular flows

Santiago Montserrat[1] · Lady Ordoñez[1,2] · Aldo Tamburrino[1,2] · Olivier Roche[3]

Received: 24 July 2020 / Accepted: 20 April 2021 / Published online: 19 May 2021

Abstract

Geophysical granular flows occur at the surface of the Earth and other planets with reduced atmospheric pressure. In this paper, we investigate the run-out of dam-break flows of particle-air mixtures with fine ($d = 75\,\mu m$) or coarse ($d = 150\,\mu m$) grains in a flume with different bottom roughness (δ) and vacuum degrees (P^*). Our results reveal an increase of the flow run-out as d/δ decreases for fine $d = 75\,\mu m$-particles, and run-out decreases with the dimensionless ambient pressure (P^*) for a given d/δ. In contrast, the run-out for coarser $d = 150\,\mu m$-particles, is almost invariant respect to P^* and d/δ. These results show that autofluidization of fine-grained flows demonstrated by earlier works at ambient pressure also occurs at reduced pressure though being less efficient. Hence, autofluidization is a mechanism, among others, to explain long run-out of geophysical flows in different environments.

Keywords Dam-break · Granular flows · Pore pressure · Ambient pressure · Fluidization · Substrate roughness

1 Introduction

The run-out distance of dense geophysical granular flows is commonly larger than expected because the apparent friction angle is significantly reduced with respect to the repose angle of same geological materials [12, 16, 21]. Friction reduction mechanisms have been attributed for instance to the formation of a low density bottom layer, caused by grains interacting with the bottom [2, 6, 11], and/or to particle-fluid interactions causing fluidization [16, 30]. However, long run-outs have been observed for flows at the surface of the Earth and celestial bodies with different gravity, substrate roughness and atmospheric conditions, the latter including the ambient atmospheric pressure, density and viscosity [20, 21, 24, 25, 33]. However, based on the analysis of Martian flows deposits, Lucas et al. [24] show that flow run-out is independent of gravity.

It is argued that friction reduction can arise because moving grains interact with the substrate, increasing random grain-velocity fluctuations at the base of the granular flow. Thus, the bulk dense flow slides over a highly agitated and low concentrated basal layer reducing the apparent basal friction [2, 6, 7, 11, 16]. Recent numerical experiments shows that the basal agitated layer can reach a height of some particles diameters and has a volume concentration as low as 0.2 [6]. However, friction reduction through this mechanism seems to occurs only for high speed flows on relatively steep substrates and bounded by lateral walls on which significant friction occurs.

Goujon et al. [14] showed experimentally that for flows of relatively large particles of size $d > 150\,\mu m$ and propagating on an inclined rough plane, the main parameter controlling flow friction was the ratio between the size of the flowing particles (d) and the size of roughness (δ). They found that flow friction was maximum at $d/\delta \sim 0.5$. They also argued

✉ Santiago Montserrat
santiago.montserrat@amtc.cl

Lady Ordoñez
lady_ordonez@hotmail.es

Aldo Tamburrino
atamburr@ing.uchile.cl

Olivier Roche
olivier.roche@uca.fr

[1] Advanced Mining Technology Center-AMTC, Universidad de Chile, Av. Tupper 2007, 8370451 Santiago, Chile

[2] Departamento de Ingeniería Civil, Universidad de Chile, Av. Blanco Encalada 2002, 8370449 Santiago, Chile

[3] Laboratoire Magmas et Volcans, Université Blaise Pascal-CNRS-IRD, OPGC Campus Universitaire des Cézeaux, 6 Avenue Blaise Pascal, TSA 60026 - CS 60026, 63178 Aubiere Cedex, France

that the increase in the flow run-out for $d/\delta <\sim 0.5$ was probably because the particles filled the substrate interstices, thus reducing the effective roughness. However, changes in flow run-out with d/δ was almost negligible for slope angles lower than $\sim$ 18°. The negligible dependence of the flow run-out with d/δ on horizontal planes was confirmed by experiments of Lube et al. [22] for $d > 300$ µm and maximum values of $d/\delta \sim 1$.

The presence of an interstitial fluid can be a key factor for friction reduction in granular flows, especially those containing high amounts of fine particles ($\sim$ 100 µm) that confer low hydraulic permeabilities [5, 10, 16, 17, 27, 28, 31]. Excess pore fluid pressure, naturally arising from upwards fluid fluxes and/or particle settling, reduces interparticle friction by locally decreasing contact forces [16, 17, 26, 27]. Excess pore fluid pressure, high above hydrostatic levels, was measured both in laboratory experiments and in natural flows in the field [16, 18, 26, 31]. Chédeville and Roche [8, 9] found that flows of fine particles on a rough substrate experienced autofluidization. This occurred as the flow particles settled into the interstices of the substrate and forced the air to escape upwards and to percolate through the flow. Autofluidization thus increased the flow run-out compared to a smooth substrate, and this effect was enhanced as the substrate roughness increased because more air was available for autofluization. On the same principle, autofluidization occurs also in collapsing beds of fine particles released from some height above a solid surface, as demonstrated by numerical simulations [5] and laboratory experiments [10]. Fine-grained mixtures can also be fluidized through mechanical vibrations that cause fluid-particle relative oscillations and related high pore fluid pressure, a phenomenon called acoustic streaming [34, 35].

Fluidization of granular flows rich in fine particles, however, is uncertain in case the atmospheric pressure is significantly lower than on Earth, as it is the case on Mars for instance (4×10^{-3}–9×10^{-3} bar). Therefore, we experimentally explore the effect of the ambient air pressure and substrate roughness on the run-out of granular flows. We perform dam-break type experiments involving different particle sizes, substrate roughness, and degrees of vacuum. To this end, we constructed a sealed channel that allowed us to make experiments up to $\sim$ 99% of vacuum relative to the ambient atmosphere. To our knowledge, this is the first investigation conducted under vacuum conditions and using fine particles. Previous granular flow experiments under high vacuum conditions were performed with coarser particles and showed no significant effects of the vacuum degree on flow emplacement [4]. Our results highlight the importance of the ambient fluid and bottom roughness in increasing flow-run out of fine particles ($d \sim 75$ µm) even at low vacuum degrees, while for coarser particles ($d \geq 150$ µm) both effects are negligible.

2 Materials and methods

We conducted dam-break experiments in a sealed lock-exchange channel 180 cm-long, 19.3 cm-wide and 50 cm-high (Fig. 1). A sluice gate separates the channel from the reservoir at the upper end, where the particles are retained. This section is 100 cm high, so that the gate can be opened inside the device. The reservoir has a length $x_o = 20$ cm. We generate granular flows by a rapid vertical release of the sluice gate (< 0.1 s). The experimental device is made of a 30 mm-thick transparent plexiglass to permit flow

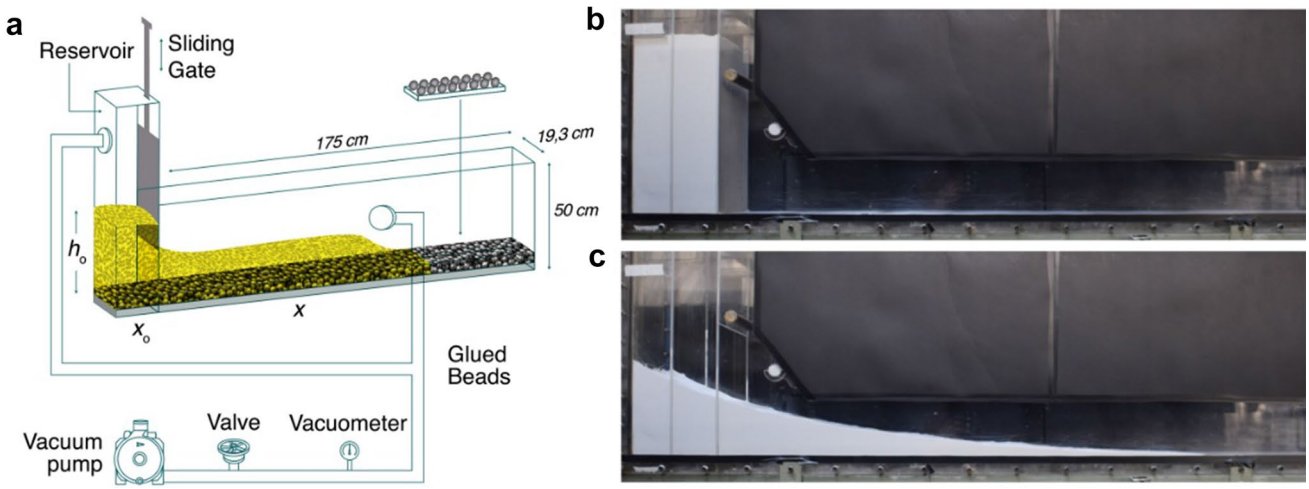

Fig. 1 **a** Sketch of the experimental device. h_o and x_o denotes the initial height and length of the column of particles inside the reservoir, respectively, while x is the flow-front position measured from the gate, **b** side view of the experimental channel before removing the gate. Particles (in white) are in the reservoir. **c** Side view of the final deposit

visualization and to resist high degrees of vacuum. It is also equipped with a vacuum pump to reduce ambient air pressure, and the degree of vacuum is measured using a *EdwardsAPG*100 − *XM* vacuometer. The maximum degree of vacuum that can be reached in the channel system is of the order of ∼ 1% of the atmospheric pressure. For the range of ambient pressures we use (1–100% of the atmospheric pressure), air viscosity remains constant [3, 4].

The bottom of the channel is covered by a 10 mm-thick aluminum sheet over which the granular flow propagates. Different roughnesses where obtained by gluing a single layer of particles of diameter δ to the aluminum base. We tested three different bottom roughness conditions: (1) aluminum roughness, (2) $\delta = 1$ mm roughness and (3) $\delta = 3$ mm roughness. Onward, the smooth aluminum roughness condition will be denoted as $\delta = 0$.

We used two different types of near spherical glass beads (Ballotini, Potters Industries) with characteristics diameters $d_1 \sim 75\,\mu$m (∼ 40 to ∼ 140 µm) and $d_2 \sim 150\,\mu$m (∼ 70 to ∼ 300 µm), repose angles $\theta_1 = 27.1° \pm 0.4°$ and $\theta_2 = 27.7° \pm 0.3°$, and both with a particle density of $\rho_p = 2500\,\text{kg/m}^3$. Particles where carefully poured inside the reservoir in order to achieve near constant mixture densities, $\rho_1 = 1360 \pm 15\,\text{kg/m}^3$ for $d \sim 75\,\mu$m-particles and $\rho_2 = 1412 \pm 6\,\text{kg/m}^3$ for $d \sim 150\,\mu$m-particles, resulting in initial particle volume concentrations $c_{v1} = 0.54 \pm 0.01$ and $c_{v2} = 0.56 \pm 0.01$ (i.e. particle-mixture porosity $\phi_1 = 0.46 \pm 0.01$ and $\phi_2 = 0.44 \pm 0.01$). Particles bed heights in the reservoir where varied from $ho \sim 20$ to $ho \sim 40$ cm (in terms of mass, from ∼ 10.5 to ∼ 22.5 kg).

In our experiments, and due to the relatively narrow grain size range of the materials, we did not expect significant particle size segregation in the reservoir, flow or deposit. Thus, segregation was neglected in our analysis. In addition, the channel width to particle size ratio was of the order of ∼ 2550 and ∼ 1280 for fine and coarse particles respectively, so that negligible sidewall effects were expected. However, side wall effects seem to be responsible in reducing flow run out in case of initial high column aspect ratios ($h_o/x_o > 1.5$) respect to low column aspect ratios [28, 32]. Nevertheless, these differences are less than the observed experimental variability and we assumed that sidewall effects had a negligible influence on our flows.

3 Results

3.1 Flow run-out distance

The run-out distance of flows of particles of size $d = 75\,\mu$m shows an important increase with both ambient pressure and substrate roughness. Figure 2 shows that, for these particles, the dimensionless flow run-out ($x_f^* = x_f/h_0$) increases fairly

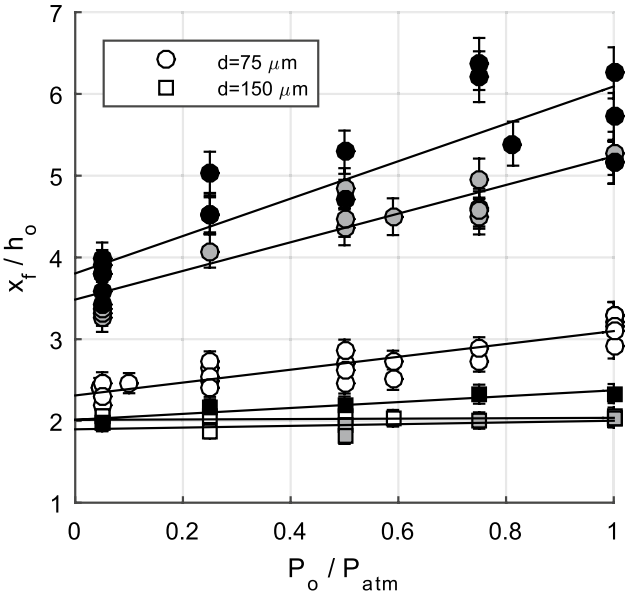

Fig. 2 Dimensionless flow run-out, x_f/h_o, as a function of the dimensionless ambient pressure P_o/P_{atm} (with P_o the ambient pressure inside the channel and P_{atm} the atmospheric pressure in the laboratory). White, gray and dark symbols represent smooth, 1 mm and 3 mm bottom roughness respectively. Note that symbols may be larger than error bars

linearly with the dimensionless ambient pressure $P* = P_o/P_{atm}$ (where P_o denotes for the ambient pressure inside the channel and P_{atm} is the atmospheric pressure in the laboratory). The dimensionless flow run-out under vacuum conditions (i.e. $P^* = 0$), inferred from the best linear fits shown in Fig. 2, increases from $x_f^* = 2.3$ to $x_f^* = 3.5$, and $x_f^* = 3.8$ for smooth, 1 mm and 3 mm-substrate roughnesses, respectively. This corresponds to a flow run-out increase of 52% and 65%, for 1 mm and 3 mm roughnesses, respectively, compared to the smooth case in the absence of an interstitial fluid. In addition, the substrate roughness increases the growth rate of the dimensionless flow run-out with the ambient pressure. While the slope of the fitted straight lines for the case of the smooth surface is 0.79, it increases to 1.75 and 2.29 for 1 mm and 3 mm-substrate roughnesses, respectively. This results in values of $x_f^* = 3.1$, $x_f^* = 5.2$ and $x_f^* = 6.1$ for smooth, 1 mm and 3mm-substrate roughnesses, respectively, at laboratory ambient conditions ($P* = 1$). This corresponds to an increase of the flow run-out of 68% and 97% for 1 mm and 3 mm-roughnesses, respectively, compared to the smooth case.

The flow run-out distance for particles of size $d = 150\,\mu$m shows to be independent of both the ambient pressure and surface roughness (Fig. 2), except for the case of $\delta = 3$ mm, where a slight increasing tendency of the flow run-out is observed with P^*. The dimensionless run-out for $d = 150\,\mu$m

particles is always significantly lower than that of flows of $d = 75\,\mu m$ particles for the same range of ambient pressure and channel roughness. Note that at vacuum conditions, the dimensionless flow run-out for $d = 75\,\mu m$ ($x_f^* = 2.3$) on a smooth substrate is slightly higher ($\sim$ 15%) than that for $d = 150\,\mu m$ ($x_f^* = 2$).

3.2 Flow-front dynamics and flow morphology of fine particle mixtures

In this section, we examine fine particles mixtures as no significant changes in the flow front dynamics and flow morphology are observed for coarser particles ($d \sim 150\,\mu m$), neither with P^* nor δ. In addition, and to simplify the analysis, we only compare the obtained results between the two roughness extremes used in the experiments (i.e. $\delta = 0$ and $\delta = 3\,mm$).

Figure 3 shows the dimensionless flow front position, $x^* = x/h_o$, for $d = 75\,\mu m$-particles, as a function of the dimensionless time, $t^* = t/(h_o/g)^{1/2}$ [30], where x denotes the horizontal flow front position measured from the gate, t is time, and g is the gravitational acceleration, for different vacuum conditions and for a smooth substrate ($\delta = 0$). The flow front propagates in three different phases, as known for flows under atmospheric pressure conditions [19, 23, 30, 36]. Under atmospheric conditions ($P^* = 1$), Figure 3 shows a first phase for which the flow front accelerates (first phase) until it reaches a constant front velocity U equal to $\alpha(gh_o)^{1/2}$, where α is a proportionality constant close to $\sim$ 1 [30]. The constant velocity phase occurs for $\sim 1.5 < t^* <\sim 3.0$. A second transition occurs at $t^* \sim 3.0$, where the flow starts decelerating until it comes to halt at $t^* \sim 5{-}5.5$.

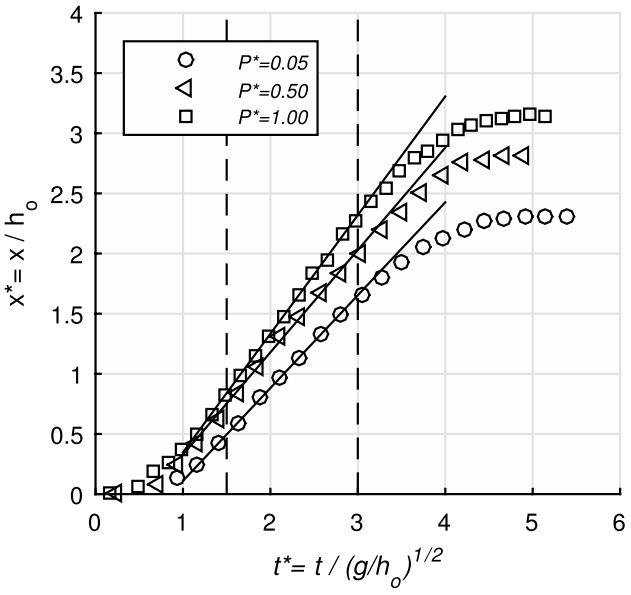

Fig. 3 Dimensionless flow front position x^* for different values of P^* and $\delta = 0$

The same trend is observed at reduced atmospheric conditions (Fig. 3), with the transitions between phases occurring at the same values of t^* than for laboratory ambient pressure (i.e. $P^* = 1$). The main effect of the ambient pressure is a velocity decrease in the constant-velocity phase, with α decreasing from $\alpha = 0.99$ at laboratory atmospheric conditions to $\alpha = 0.85$ and $\alpha = 0.77$ at $P^* = 0.50$ and $P^* = 0.05$, respectively.

Figure 4 shows that the front position for fine particles flows ($d = 75\,\mu m$) at $\delta = 0$ and $\delta = 3\,mm$ and different vacuum degrees are almost identical until $t^* \sim 3.0$. However, for rough substrates ($\delta = 3\,mm$), the constant velocity phase lasts longer. For example, for $\delta = 3\,mm$, the transition between the second and third phase occurs at $t^* \sim 5$. In addition, increasing roughness significantly reduces the front deceleration, thus increasing the flow run-out and duration [8, 9]. While flows on a smooth substrate stop at $t^* \sim 5 - 5.5$, almost independently of P^*, at $\delta = 3\,mm$ flow duration last up to $t^* \sim 7$, $t^* \sim 8$ and $t^* \sim 9$ for $P^* = 0.05$, $P^* = 0.50$ and $P^* = 1.00$, respectively.

These kinematics can be complemented considering the flow morphology, which varies very little with the channel roughness until the end of the constant velocity phase for smooth surfaces ($t^* \sim 3$), regardless of $P*$ (Fig. 5). For $t^* > 3$, the flow length increases with the substrate roughness, because a thin flow head arises from the flow body, even after the latter has stopped [8]. Slight differences in the position of the center of area (equivalent to the center of mass in 3D) of the flow for smooth and 3 mm rough surfaces confirm that the increasing flow length with roughness is due to the very thin frontal part of the flow that propagates downstream and causes long run-out.

4 Discussion

Sustained high pore fluid pressure has been pointed out as one of the primary friction reduction mechanisms in experimental flows of initially fluidized fine ($<\sim 100\,\mu m$) granular materials propagating on smooth or rough surfaces at earth atmospheric conditions [5, 8–10, 27, 28, 30, 31]. Notice that initially non-fluidized flows with shorter run-out distances have the ability to self-generate excess pore fluid pressure to near $\sim$ 15% of the weight of the particle, possibly because of granular mixture compaction [31] or by air incorporation at the flow front [1]. However, this last mechanism has shown to be negligible in experimental flows [9]. Recent dam-break experiments show that the mixture porosity is correlated with flow velocity as it decreases during flow acceleration (i.e. mixture dilation) and increases during flow deceleration (i.e. mixture compaction) [36]. In case of

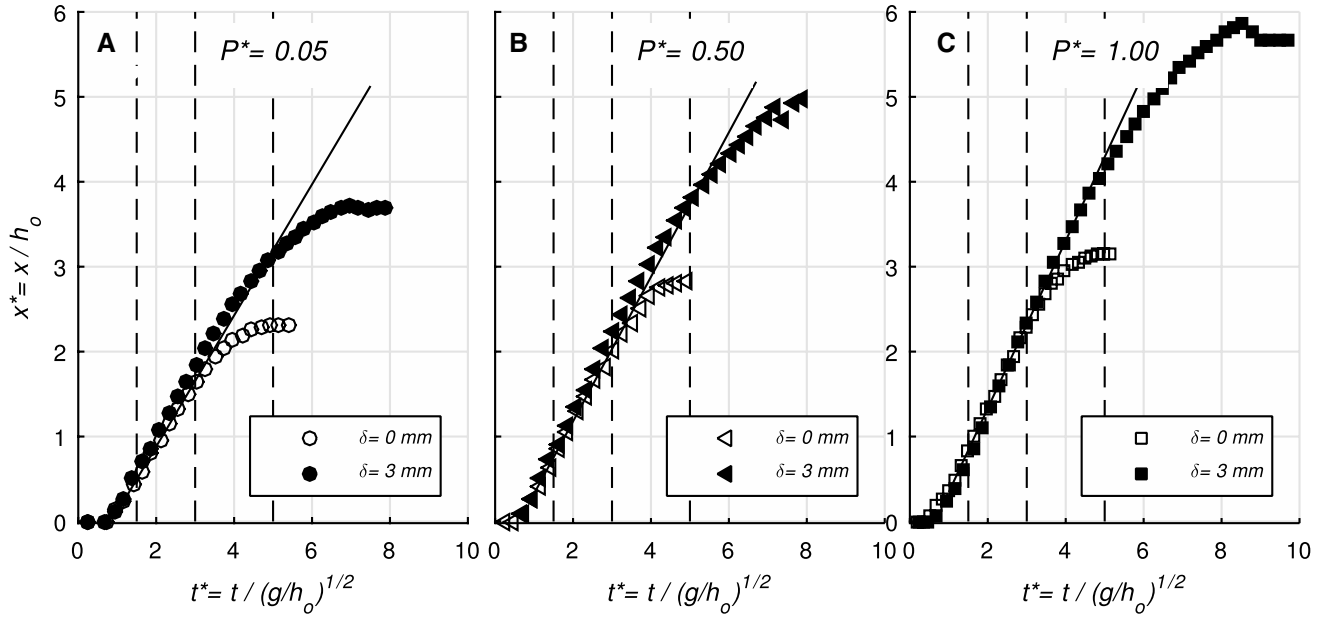

Fig. 4 Dimensionless flow front position, x^*, for different values of P^* and δ, for fine 75 μm particles

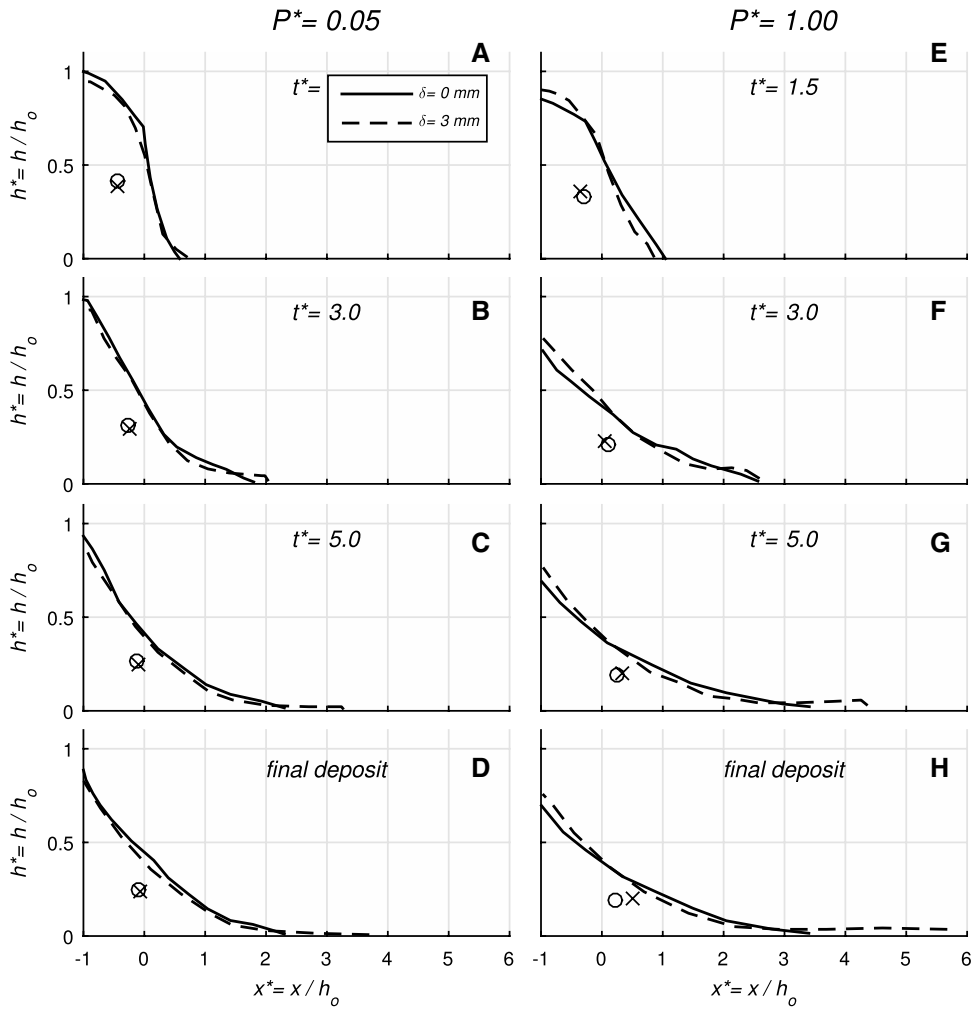

Fig. 5 Flow morphology for different δ and P^*. ∘ and × denotes for the center of area of the flowing mixture for $\delta = 0$ and $\delta = 3$ mm, respectively

granular compaction, pore pressure rises by the compression of air trapped in the interstices if the time scale for particles rearrangement (T_R) is small compared with the time scale for vertical pore pressure diffusion (T_D) [15]. The opposite occurred in case of mixture dilation (i.e. pore pressure drops when the mixture and pores dilate). For a given change in air volume (ΔV_a), and assuming isothermal air compression, the upper limit for pore pressure variations (ΔP) respect to the ambient pressure (P_o) can be approximated as [15]:

$$\Delta P = -P_o \frac{\Delta V_a}{V_a} \tag{1}$$

where V_a is the volume of air in the interstices and ΔV_a is defined positive for air dilation and negative for air compression. In Eq. (1), non linear terms have been neglected [15].

As $P_o = P^* P_{atm}$, Eq. (1) shows that for similar changes in the air volume between grains, $|\Delta P|$ linearly decreases with the degree of vacuum ($\Delta P \sim P^*$). Thus, autofluidization is possible even under reduced atmospheric conditions, and decreasing the ambient pressure will linearly decrease the amount of pore pressure changes. This can explain the observed linear trends between the flow run-out and the degree of vacuum ($x_f/h_o \sim P^*$, see Fig. 2), at least for the case $\delta = 0$ and $d = 75$ µm-particles. In this sense, reducing P_o increases the effective flow friction, which also agrees with the observed reductions in flow duration and flow-front velocities during the constant velocity phase.

For flows over rough substrates ($\delta = 1$ mm and $\delta = 3$ mm), fluidization can arise because of particles falling into the substrate interstices and forcing the air to percolate upwards through the granular flow [8, 9]. The amount of pore fluid pressure due to drag interactions (Δp) increases with air velocity and can be accounted in packed beds by the semi-empirical Ergun equation [13], here expressed in terms of the degree of fluidization ($\Delta p^* = \Delta p / P_L$) of a granular column of height h and bulk density ρ:

$$\Delta p^* = \frac{\Delta p}{P_L} = 150 \frac{\mu_g U_g}{\rho g d^2} \frac{(1-\phi)^2}{\phi^3} + 1.75 \frac{\rho_g U_g^2}{\rho g d} \frac{1-\phi}{\phi^3} \tag{2}$$

where μ_g is the gas dynamic viscosity, U_g is the superficial gas velocity (defined as the flow rate per unit cross sectional area), ρ_g is the gas density and ϕ is the particle-mixture porosity (defined previously). We assumed that changes of porosity was negligible during flow emplacement, making the Ergun equation relevant for describing fluidization. The first and second terms at the right-hand of Eq. 2 accounts for viscous and inertial fluidization, respectively.

$\Delta p^* = 1$ means that the entire weight of the particle bed is supported by air drag, which occurs at a minimum value of U_g called the minimum fluidization velocity, U_{mf}. Solving Eq. 2 for $\Delta p^* = 1$ results in $U_{mf} = 11$ mm/s and $U_{mf} = 32$ mm/s for $d = 75$ µm and $d = 150$ µm-particles, respectively. These values scale with previous experimental measurements done on similar materials [29]. Chédeville and Roche [8] estimate that particles falling into the interstices generate upward air fluxes above U_{mf}-values due to the high settling velocities of the particles. For the estimated values of U_{mf}, the first term on the right hand side of Eq. 2 is ~ 1, while the second term is $\sim 10^{-3}$, meaning that fluidization is mainly due to viscous drag. Thus, for the range of P-values used for this experiments, for which μ is constant, autofluidization related to a rough substrate is always possible, even at high vacuum conditions. This explains the increasing run-out of $d = 75$ µm-particles mixtures compared to a smooth substrate even at very low ambient pressure conditions ($P^* \sim 0.05$). *Umf* for $d = 150$ µm-particles is larger than for $d = 75$ µm-particles. As both types of particles fall into the interstices as about the same velocity, then the interstitial air velocity should be in the same order in both cases. However, this result in smaller Δp^* for $d = 150$ µm-particle mixtures, explaining the almost null effect of P^* in the run-out of these flows. The slight increase of x_f^* with P^* observed for $\delta = 3$ mm, suggests that higher volumes of air trapped into the interstices are able to sustain vertical air fluxes for longer periods, promoting a weak fluidization compared with $d = 75$ µm-particles flows.

An alternative (or complementary) friction reduction mechanism, consisting in the development of a low density layer at the flow bottom because of flow particles colliding with those of the bottom roughness, may also be considered. In this context, the flow run-out is expected to be a function of d/δ [14]. In the case of a smooth surface (aluminum substrate) we assume $d/\delta = 1$, as it has been observed that the flow rides over a thin layer of the same particles deposited after the passage of the flow-front [22]. Thus, for $d = 75$ µm -particles $d/\delta = 1 - 0.025$, while for $d = 150$ µm-particles $d/\delta = 1 - 0.05$. Although d/δ varies in a similar range for both types of particles, the flow run-out with d/δ for $d = 150$ µm-particles does not vary significantly. This suggests that viscous fluidization controls the flow mechanism of fine granular mixtures and confirms that, in the absence of autofluidization, d/δ does not control the flow run-out in horizontal channels.

5 Conclusions

Our results confirm that viscous air-particle interactions are an important friction reduction mechanism for fine-grained granular flows. In our experiments, the relative increase of flow run-out with the substrate roughness is reduced as the ambient pressure decreases, but such increase is still significant (65%, from $\delta = 0$ to 3 mm) even at $P^* = 0.05$ (Fig. 2). This suggests that the autofluidization mechanism acting

in flows of fine particles on rough substrate and at atmospheric pressure [8, 9] operates as well at lower pressures. This can be explained because viscosity remains constant for the range of vacuum conditions explored in this study and because, for particles of this size range, fluidization is dominated by fluid viscosity [3, 30].

The above-mentioned friction reduction mechanisms does not act for coarser particle materials ($d \sim 150\,\mu m$). This can be explained as the air initially present in the substrate interstices is expelled upwards at lower velocities compared with the minimum fluidization velocity (U_{mf}) of the coarse particles (see Chédeville and Roche [8] for experiments at $P^* = 1$) or because the amount of air trapped in the interstices is not enough to fluidize the particle mixture over a significant duration. An exception occurs for $\delta = 3$ mm, where a slight influence of P^* in the flow run-out is observed. In addition, for coarser $d \sim 150\,\mu m$-particles, the increasing roughness does not have significant effects on the flow run-out, even for a similar range of d/δ compared with $d = 75\,\mu m$-particles flows. Thus, in the absence of fluidization capacity of the flowing mixture, increasing roughness shows not to be an important friction reduction mechanism in granular flows. However, this mechanism could become important for high-velocity flows on steep substrates [6].

Regarding the motion of the flow front of fine-grained mixtures, decreasing the ambient pressure mainly results in a decrease in velocity and duration of the constant velocity phase. This is a consequence of the reduction of the autofluidization capacity, proportional to $|\Delta P|$, which causes increasing friction. Increasing δ increases the flow run-out by increasing the time of the constant velocity phase and the stopping phase. This is because, for larger δ, the air is expelled from the substrate for longer duration as more air is trapped initially in their interstices. However, the increase in flow run-out is due to a thin flowing frontal layer that spreads from the flow body at $t^* \sim 3$, which represents a little amount of the total mass. Thus, the run-out of the bulk flow, represented by the run-out of the center of area of the avalanche (see Fig. 5), is almost independent of d/δ.

Our findings have implications for granular mass flows on extraterrestrial planets with reduced atmospheric pressure. They suggest that fluidization caused by viscous drag may occur through vertical gas fluxes within the granular flow, even at low ambient pressure. This is likely to occur when flows propagating on rough substrates contain high amounts of fine particles that settle into the substrate interstices. However, fluidization may also arise from air compression (i.e. increasing pore pressure) during fast contraction of the particle network. This second mechanism decreases when reducing the atmospheric pressure, thus increasing flow friction and reducing the flow run-out. This is likely to be important for fine particle flows, where the time for particle rearrangements is small compared with the time for pore pressure diffusion

Acknowledgements This work was supported by the Advanced Mining Technology Center (AMTC) and Departamento de Ingeniería Civil, form Universidad de Chile, the French National Research Institute for Sustainable Development (IRD, France) and the Chilean National Commission for Scientific and Technological Research, CONICYT, through Fondecyt Projects 1130910 and 11130254 and PIA Project AFB180004. We thank P. Mendoza and two anonymous reviewers for helpful comments on our work. We also thank C. González for his assistance with graphics. This is Laboratory of Excellence ClerVolc Contribution No. 481.

Declarations

Conflict of interest The authors declare that they have no conflict of interest.

References

1. Bareschino, P., Lirer, L., Marzocchella, A., Petrosino, P., Salatino, P.: Self-fluidization of subaerial rapid granular flows. Powder Technol. **182**(3), 323–333 (2008). https://doi.org/10.1016/j.powtec.2007.12.010
2. Bartelt, P., Buser, O., Platzer, K.: Fluctuation dissipation relations for granular snow avalanches. J. Glaciol. **52**(179), 631–643 (2006). https://doi.org/10.3189/172756506781828476
3. Bello, I.: Vacuum and Ultravacuum. CRC Press, London (2017). https://doi.org/10.1201/9781315155364
4. Börzsönyi, T., Ecke, R.E.: Rapid granular flows on a rough incline: phase diagram, gas transition, and effects of air drag. Phys. Rev. E **74**(6), 61301 (2006). https://doi.org/10.1103/PhysRevE.74.061301
5. Breard, E.C.P., Dufek, J., Lube, G.: Enhanced mobility in concentrated pyroclastic density currents: an examination of a self-fluidization mechanism. Geophys. Res. Lett. **45**(2), 654–664 (2018). https://doi.org/10.1002/2017GL075759
6. Brodu, N., Delannay, R., Valance, A., Richard, P.: New patterns in high-speed granular flows. J. Fluid Mech. **769**, 218–228 (2015). https://doi.org/10.1017/jfm.2015.109
7. Campbell, C.S.: Self-lubrication for long runout landslides. J. Geol. **1989**, 653–665 (1989). https://doi.org/10.1086/629350
8. Chedeville, C., Roche, O.: Autofluidization of pyroclastic flows propagating on rough substrates as shown by laboratory experiments. J. Geophys. Res. Solid Earth **119**(3), 1764–1776 (2014). https://doi.org/10.1002/2013JB010554
9. Chédeville, C., Roche, O.: Influence of slope angle on pore pressure generation and kinematics of pyroclastic flows: insights from laboratory experiments. Bull. Volcanol. **77**(11), 96 (2015). https://doi.org/10.1007/s00445-015-0981-4
10. Chédeville, C., Roche, O.: Autofluidization of collapsing bed of fine particles: implications for the emplacement of pyroclastic flows. J. Volcanol. Geoth. Res. **368**, 91–99 (2018). https://doi.org/10.1016/j.jvolgeores.2018.11.007
11. Cleary, P.W., Campbell, C.S.: Self-lubrication for long runout landslides: examination by computer simulation. J. Geophys. Res. Solid Earth **98**(B12), 21911–21924 (1993). https://doi.org/10.1029/93JB02380
12. Delannay, R., Valance, A., Mangeney, A., Roche, O., Richard, P.: Granular and particle-laden flows: from laboratory experiments to

field observations. J. Phys. D: Appl. Phys. **50**(5), 053001 (2017). https://doi.org/10.1088/1361-6463/50/5/053001
13. Gibilaro, L.G.: Fluidization Dynamics. Elsevier, London (2001)
14. Goujon, C., Thomas, N., Dalloz-Dubrujeaud, B.: Monodisperse dry granular flows on inclined planes: role of roughness. Eur. Phys. J. E **11**(2), 147–157 (2003). https://doi.org/10.1140/epje/i2003-10012-0
15. Homan, T., Gjaltema, C., van der Meer, D.: Collapsing granular beds: the role of interstitial air. Phys. Rev. E **89**(5), 052204 (2014). https://doi.org/10.1103/PhysRevE.89.052204
16. Iverson, R.M.: The physics of debris. Rev. Geophys. **35**(97), 245–296 (1997). https://doi.org/10.1029/97RG00426
17. Iverson, R.M., Denlinger, R.P.: Flow of variably fluidized granular masses across three-dimensional terrain: 1. Coulomb mixture theory. J. Geophys. Res. Solid Earth **106**(B1), 537–552 (2001). https://doi.org/10.1029/2000JB900329
18. Iverson, R.M., Logan, M., LaHusen, R.G., Berti, M.: The perfect debris flow? Aggregated results from 28 large-scale experiments. J. Geophys. Res. Earth Surf. (2010). https://doi.org/10.1029/2009JF001514
19. Lajeunesse, E., Monnier, J.B., Homsy, G.M.: Granular slumping on a horizontal surface. Phys. Fluids **17**(103), 302 (2005). https://doi.org/10.1063/1.2087687
20. Lajeunesse, E., Quantin, C., Allemand, P., Delacourt, C.: New insights on the runout of large landslides in the Valles-Marineris canyons, Mars. Geophys. Res. Lett. (2006). https://doi.org/10.1029/2005GL025168
21. Legros, F.: The mobility of long-runout landslides. Eng. Geol. **63**(3), 301–331 (2002). https://doi.org/10.1016/S0013-7952(01)00090-4
22. Lube, G., Huppert, H.E., Sparks, R.S.J., Hallworth, M.A.: Axisymmetric collapses of granular columns. J. Fluid Mech. **508**(1), 175–199 (2004). https://doi.org/10.1017/S0022112004009036
23. Lube, G., Huppert, H.E., Sparks, R.S.J., Freundt, A.: Collapses of two-dimensional granular columns. Phys. Rev. E **72**(4), 041301 (2005). https://doi.org/10.1103/PhysRevE.72.041301
24. Lucas, A., Mangeney, A.: Mobility and topographic effects for large Valles Marineris landslides on Mars. Geophys. Res. Lett. **34**(10), L10201 (2007). https://doi.org/10.1029/2007GL029835
25. Lucas, A., Mangeney, A., Ampuero, J.P.: Frictional velocity-weakening in landslides on Earth and on other planetary bodies. Nat. Commun. (2014). https://doi.org/10.1038/ncomms4417
26. McArdell, B.W., Bartelt, P., Kowalski, J.: Field observations of basal forces and fluid pore pressure in a debris flow. Geophys. Res. Lett. (2007). https://doi.org/10.1029/2006GL029183
27. Montserrat, S., Tamburrino, A., Roche, O., Niño, Y.: Pore fluid pressure diffusion in defluidizing granular columns. J. Geophys. Res. **117**(F2), F02034 (2012). https://doi.org/10.1029/2009JB007133
28. Montserrat, S., Tamburrino, A., Roche, O., Niño, Y., Ihle, C.F.: Enhanced run-out of dam-break granular flows caused by initial fluidization and initial material expansion. Granul. Matter **18**(1), 1–9 (2016). https://doi.org/10.1007/s10035-016-0604-6
29. Roche, O., Gilbertson, M.A., Phillips, J.C., Sparks, R.S.J.: Experimental study of gas-fluidized granular flows with implications for pyroclastic flow emplacement. J. Geophys. Res. Solid Earth (2004). https://doi.org/10.1029/2003JB002916
30. Roche, O., Montserrat, S., Niño, Y., Tamburrino, A.: Experimental observations of water-like behavior of initially fluidized, dam break granular flows and their relevance for the propagation of ash-rich pyroclastic flows. J. Geophys. Res. **113**(B12), B12203 (2008). https://doi.org/10.1029/2008JB005664
31. Roche, O., Montserrat, S., Niño, Y., Tamburrino, A.: Pore fluid pressure and internal kinematics of gravitational laboratory air-particle flows: insights into the emplacement dynamics of pyroclastic flows. J. Geophys. Res. **115**(B09), 206 (2010). https://doi.org/10.1029/2009JB007133
32. Roche, O., Attali, M., Mangeney, A., Lucas, A.: On the run-out distance of geophysical gravitational flows: insight from fluidized granular collapse experiments. Earth Planet. Sci. Lett. **311**(3), 375–385 (2011). https://doi.org/10.1016/j.epsl.2011.09.023
33. Singer, K.N., McKinnon, W.B., Schenk, P.M., Moore, J.M.: Massive ice avalanches on Iapetus mobilized by friction reduction during flash heating. Nat. Geosci. **5**(8), 574–578 (2012). https://doi.org/10.1038/ngeo1526
34. Soria-Hoyo, C., Valverde, J.M., Roche, O.: A laboratory-scale study on the role of mechanical vibrations in pore pressure generation in pyroclastic materials: implications for pyroclastic flows. Bull. Volcanol. **81**(2), 12 (2019). https://doi.org/10.1007/s00445-019-1271-3
35. Valverde, J.M., Soria-Hoyo, C.: Vibration-induced dynamical weakening of pyroclastic flows: insights from rotating drum experiments. J. Geophys. Res. Solid Earth **120**(9), 6182–6190 (2015). https://doi.org/10.1002/2015JB012317
36. Xu, X., Sun, Q., Jin, F., Chen, Y.: Measurements of velocity and pressure of a collapsing granular pile. Powder Technol. **303**, 147–155 (2016). https://doi.org/10.1016/j.powtec.2016.09.036